Three-dimensional multilevel memory based on laser-polarization-dependence birefringence

Guanghua Cheng (程光华)[1], Qing Liu (刘 青)[1,2], Yishan Wang (王屹山)[1], Wei Zhao (赵 卫)[1], and Guofu Chen (陈国夫)[1]

[1]*State Key Laboratory of Transient Optics and Photonics, Xi'an Institute of Optics and Precision Mechanics, Chinese Academy of Sciences, Xi'an 710068*

[2]*Applied Physics institute, Zhejiang Wanli College, Ningbo 315101*

Received June 17, 2005

The femtosecond laser-modified region in isotropic glass medium shows a big optical birefringence. Transmission of the birefringent regions between two crossed polarizers depends on phase retardation and the orientation angle of the birefringent optical axes. Based on this effect, three-dimensional (3D) multilevel memory was proposed and demonstrated for nonvolatile memory up to eight levels, in contrast to the standard two-level technology. Eight-level writing and reading are distinguishable in fused silica with a near-infrared femtosecond laser. The retention of this memory is characterized for nonvolatile applications.

OCIS codes: 210.0210, 320.7120, 260.1440.

When an intense femtosecond pulse laser is focused inside a bulk transparent material, the intensity in the focal volume can become high enough to cause absorption through nonlinear processes, leading to alter the structure of bulk transparent material and cause a refractive index change. This ability to create three-dimensional (3D) objects with sub-micrometer precision may be useful for 3D storage which firstly reported by Glezer in 1996[1]. Pursuing a higher writing density is one of very important theme. In some papers, high numerical aperture (NA) objective even solid or liquid immersion was employed to achieve terabits/cm^3 in transparent materils[2−4]. On the other hand, those combination techniques absorb more attention because they can achieve an extreme capacity. For example, ultrashort-laser-pulse 3D memory combining with spectral hole-burning (SHB) and holograph data memory can achieve a more higher writing density (decuple increase compared with 3D memory)[5−8].

Multilevel (ML) memory technique can increase the capacity by a factor of 2 at least and native data transfer speed by a factor of 10 while ensuring backward and forward compatibility[9,10]. Following a route similar to that used in one-dimensional (1D) conventional optical storage could lead to a further increase in capacity by the addition of another dimension to writing data, such as the use of multiple levels instead of the two levels (pit and land) used in the binary two-dimensional (2D) optical storage disk format. Recently, it is developed by Calimetrics Inc and other groups in the world[11].

In this paper, we demonstrate permanent ML optical recording in 3D with an infrared femtosecond laser. The physical mechanism is based on the fact that laser-induced regions possess optical birefringence and this birefringence can be controlled by the polarization direction of the femtosecond laser. By tuning incident laser polarization direction, we present a four-level and eight-level optical recording in 3D in fused silica.

The laser used in this experiment was a regeneratively amplified Ti:sapphire femtosecond pulsed laser, had a 150-fs pulse width and 1-kHz pulse repetition rate. The microfabrication system is described in elsewhere[12]. Simply, the energy of the pulse could be varied by the combination of a quarter-wave plate and a Glan-Taylor polarizer. The energy was monitored by power meter (Coherence, field check). A laser of 32-μW (considering 35% transmission of the focusing objective) average power was focused inside the glass using a long-working-distance microscope objective (Mitutoyo, 50×, NA = 0.55). The glass sample was moved by a computer-controlled three-axis translation stage with 100-nm resolution (Physik Instrumente, German). After laser writing, the samples were evaluated using a transmission microscope (Olympus BX51, Japan). Two crossed polarizers were inserted on both sides of the sample. The transmitted light through the samples was captured by a digital camera attached to the transmission microscope viewer.

The fused silica plate (20 × 20 × 2 (mm)) on six optical surfaces was mounted on a motorized xy translation stage with linearly controlled motion along the z direction to adjust the focus of the laser inside the glass. The laser was focused approximately 226 μm below the surface of the glass plates. Each bit was excited with 5-second exposure time, according to 5000 pulses. After an exposure, the Glan-Taylor polarizer was rotated to an expected angular, accordingly, the quarter-wave quarter plate was rotated to obtain a same exposure energy. The spatial distribution of the photo-induced anisotropy is easily observed by illuminating the sample with polarized white light from the rear and observation through a rotatable linear polarizer. The birefringence is checked with Olympus BX51 optical microscopy under birefringence mode. Optical setup for reading of multilevel data stored by employing permanent photo-induced anisotropy in fused silica is shown in Fig. 1.

The data recorded in fused silica are represented through the angular orientation of permanent photo-induced anisotropy and the refractive index changes, respectively. In the previous report[2,3], without the

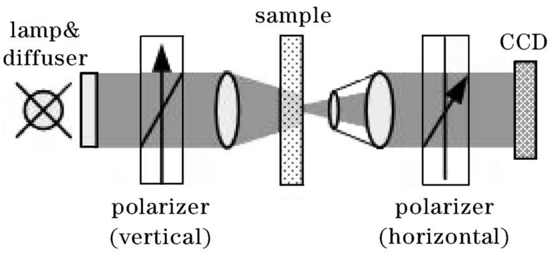

Fig. 1. Schematic of optical setup for reading of multilevel stored data.

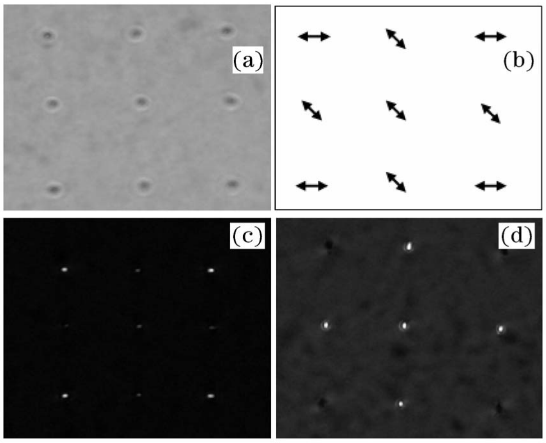

Fig. 2. Optical images of bits in fused silica induced by linearly polarized femtosecond laser pulses.

use of a polarizer, the spots where data were recorded are detectable through the change in their refractive index/optical scattering/photoluminescence. Considering that laser-modified region possesses birefringence, we change the polarization of the writing laser. In this experiment, digital zeros as well as ones are recorded through a photo process which leads to an identical refractive index change, but the only difference is the orientation angle of the birefringent optical axes, which cannot be detected by optical microscopy under transmission mode without polarizer. Figure 2 shows a transmission image (through z or the laser beam direction) of femtosecond laser modified regions in fused silica. Figure 2(a) is permanent photo-induced refractive index change in fused silica observed by optical microscopy in transmission mode without crossed polarizers. The distance between two bits is 10 μm in average. Figure 2(b) shows the polarization directions of the writing laser, Fig. 2(c) is observed spots through crossed polarizers at 0°, Fig. 2(d) is at 45°. The experimental results are consistent with the one described by Yang *et al.*[13].

The optical transmission (T) of the laser-induced birefringent bit between two crossed polarizers depends on the angle (θ) between the ordinary direction of the birefringent material and the polarization axis of the first polarizer. $T = 0.5\sin^2(2\theta)[1-\cos(\Delta nkd)]$, where Δn is birefringence, k is wave vector, and d is the thickness of the birefringent region through which the light travels. From this expression, one data stream is written with same energy, same exposure time, and different polarization direction, the optical transmission will be different under polarization mode, as shown in Fig. 3(b).

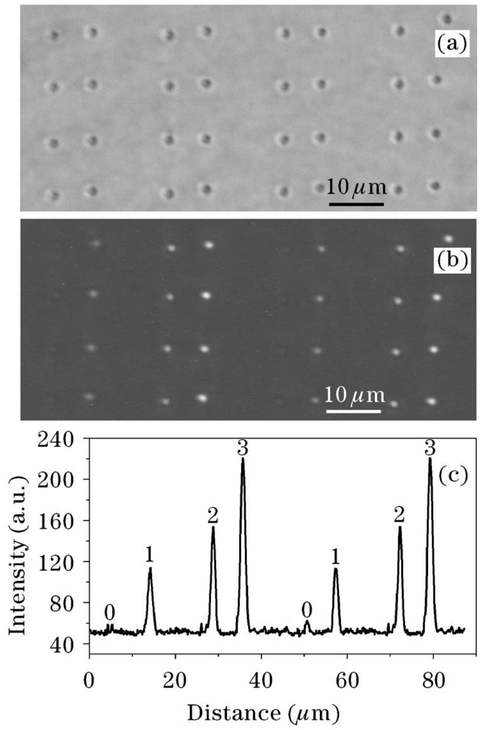

Fig. 3. The bits in fused silica written by linearly polarized femtosecond laser at 0°, 15°, 30°, and 45° polarization direction (reference to table level), respectively.

The polarization directions of the writing laser are 0°, 15°, 30°, and 45°, the transmission intensity is four-level accordingly. Based on this principle, we can realize four-level writing/reading in 3D in fused silica. Figure 3(a) is an optical microscope image without polarizers. The pixel pitch is 10 μm throughout all images. The storage density employed is far from the maximal achievable optical and materials resolution. Figure 3(b) is an optical microscope image where the sample is positioned between crossed polarizers. And Fig. 3(c) is transmission intensity of birefringent bits according to Fig. 3(b). The memory states "0", "1", "2", and "3" are written by polarization directions of 0°, 15°, 30°, and 45°, respectively.

We have further carried out writing/reading operations at eight-level as shown in Fig. 4. The polarization directions are 0°, 11°, 16.2°, 20.4°, 24.5°, 28.9°, 33.9°, and 45°, respectively, according to those intensities of 0, $\frac{1}{7}$, $\frac{2}{7}$, $\frac{3}{7}$, $\frac{4}{7}$, $\frac{5}{7}$, $\frac{6}{7}$, and 1. Due to angle error, the intensities deviate a little from the theoretical simulation. All levels were distinguishable in the tested cycles. Figure 4(a) shows an optical microscope image under transmission mode without crossed polarizer. Figure 4(b) is observed with a crossed polarizer. And Fig. 4(c) is transmission intensity of birefringent bits according to Fig. 4(b). The memory states "0", "1", "2", "3", "4", "5", "6", and "7" are written.

The optical elements fabricated by linearly polarized femtosecond laser show anisotropic characteristics, such as anisotropic photo-electronics[14], elliptical refractive index change cross-section[15], anisotropic reflection[16], and birefringence[17]. Some characteristics can attributed to the polarization electronic field of the irradiated

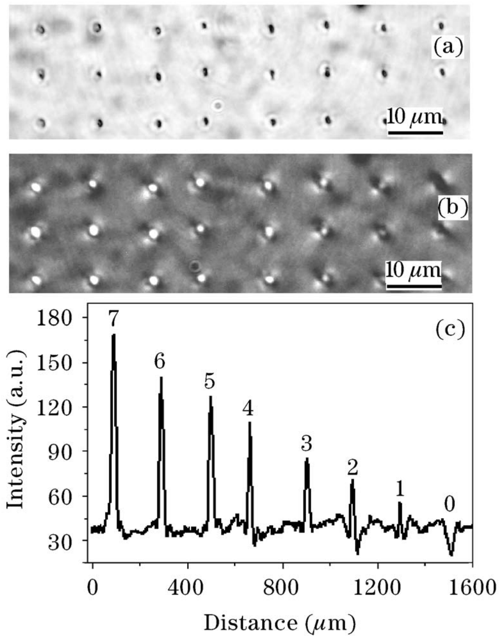

Fig. 4. Eight-level optical writing with linearly polarized laser at 0°, 11°, 16.2°, 20.4°, 24.5°, 28.9°, 33.9°, and 45°, respectively.

femtosecond laser pulse. However, the fundamental mechanisms that create the birefringence in the bulk glass by femtosecond laser irradiation are not yet clear. The dependence of birefringence on polarization shows that the optical birefringence cannot be solely attributed to a thermal effect generated by multiphoton absorption or plasma formation. If a thermal-heating effect is a major contributor, the laser-modified region should be optically isotropic.

There are two possible mechanisms contributed to the birefringence in the irradiated region. One is crystallization in laser-irradiated region, these phenomena described by Gorelik[18] are that multi-shot irradiated region results in partial crystallization of the amorphous core, viewing by transmission electron microscopy. Photo-thermo-refractive (PTR) glass[19] can crystallize after irradiation with femtosecond laser pulse and followed by a thermal development. So we hoped to check this kind of material for monitoring birefringence and crystallization. However, it failed and no birefringence was observed after irradiation and thermal development, just crystallization happened.

The other one is high-spatial-frequency (HSF) gratings[20] in silica glass irradiated by ultrashort light pulses[15]. However, electron plasma density wave is just coupled with the incident laser field at the direction of laser propagation. The coupling is increased by a periodic structure created via a pattern of interference between the incident light field and the electric field of the bulk electron plasma wave, resulting in the periodic modulation of the electron plasma concentration and the structural changes in glass. If the incident laser is circle polarization, the periodic modulation would disappear. No birefringence is observed in circular-polarized laser-irradiated region. It is consistent with our observation in experiment. Considering the difficulty at the sample preparation and expensive cost, it is not been checked whether there have nanograting in circular-polarized laser-irradiated region.

In conclusion, based on the fact that laser-induced regions possess optical birefringence and this birefringence can be controlled by the polarization direction of the femtosecond laser, we demonstrated four-level and eight-level optical memories in 3D in fused silica with a linearly polarized femtosecond laser pulse. Our multilevel data stored in 3D represents a conceptual breakthrough in femtosecond laser memory.

This work was supported by the Innovation Foundation of Chinese Academy of Sciences (No. 40001043). G. Cheng's e-mail address is gcheng@opt.ac.cn.

References

1. E. N. Glezer, M. Milosavljevic, L. Hung, R. J. Finlay, T.-H. Her, J. P. Callan, and E. Mazur, Opt. Lett. **21,** 2023 (1996).
2. G. Cheng, Y. Wang, J. D. White, Q. Liu, W. Zhao, and G. Chen, J. Appl. Phys. **94,** 1304 (2003).
3. F. He, G. Cheng, D. Zhang, and X. Feng, Chin. Opt. Lett. **2,** 423 (2004).
4. M. Nakano, T. Kooriya, T. Kuragaito, C. Egami, Y. Kawata, M. Tsuchimori, and O. Watanabe, Appl. Phys. Lett. **85,** 176 (2004).
5. J. Qiu and K. Hirao, J. Mater. Sci. Lett. **20,** 691 (2001).
6. J. Qiu, K. Nouchi, K. Miura, T. Mitsuyu, and K. Hirao, J. Phys.: Condens. Matter **12,** 5061 (2000).
7. K. Holiday, M. Croci, E. Vauthey, and U. P. Wild, Phys. Rev. B **47,** 14741 (1993).
8. J. H. Stricker and W. W. Webb, Opt. Lett. **16,** 1780 (1991).
9. L. Fagoonee, W. Coene, A. Moinian, and B. Honary, Opt. Lett. **29,** 385 (2004).
10. C. Li, W. Fan, B. Lei, D. Zhang, S. Han, T. Tang, X. Liu, Z. Liu, S. Asano, M. Meyyappan, J. Han, and C. Zhou, Appl. Phys. Lett. **84,** 1949 (2004).
11. H. Hieslmair, J. Stinebaugh, T. Wong, M. O'Neill, M. Kuijper, and G. Langereis, Jpn. J. Appl. Phys. **42,** 1074 (2003).
12. G. Cheng, J. D. White, Q. Liu, Y. Wang, W. Zhao, and G. Chen, Chin. Phys. Lett. **20,** 1283 (2003).
13. P. Yang, G. R. Burns, J. Guo, T. S. Luk, and A. G. Vawter, J. Appl. Phys. **95,** 5280 (2004).
14. P. G. Kazansky, H. Inouye, T. Mitsuyu, K. Miura, J. Qiu, and K. Hirao, Phys. Rev. Lett. **82,** 2199 (1999).
15. K. Yamada, W. Watanabe, J. Nishii, and K. Itoh, J. Appl. Phys. **93,** 1889 (2003).
16. J. D. Mills, P. G. Kazansky, E. Bricchi, and J. J. Baumberg, Appl. Phys. Lett. **81,** 196 (2002).
17. G. Cheng, Q. Liu, Y. Wang, L. Yu, W. Zhao, and G. Chen, Chin. Opt. Lett. **2,** 119 (2004).
18. T. Gorelik, M. Will, S. Nolte, A. Tuennermann, and U. Glatzel, Appl. Phys. A **76,** 309 (2003).
19. Y. Cheng, K. Sugioka, M. Masuda, K. Shihoyama, K. Toyoda, and K. Midorikawa, Opt. Express **11,** 1809 (2003).
20. I. Richter, P. Sun, F. Xu, and Y. Faimman, Appl. Opt. **34,** 2421 (1995).